Molecules and Cells

Endoplasmic Reticulum Stress Induces CAP2 Expression Promoting Epithelial-Mesenchymal Transition in Liver Cancer Cells

Sarah Yoon[1,2], Boram Shin[1,2], and Hyun Goo Woo[1,2,*]

[1]Department of Physiology, Ajou University School of Medicine, Suwon 16499, Korea, [2]Department of Biomedical Science, Graduate School, Ajou University, Suwon 16499, Korea
*Correspondence: hg@ajou.ac.kr
https://doi.org/10.14348/molcells.2021.0031
www.molcells.org

Cyclase-associated protein 2* (*CAP2*) has been addressed as a candidate biomarker in various cancer types. Previously, we have shown that *CAP2* is expressed during multi-step hepatocarcinogenesis; however, its underlying mechanisms in liver cancer cells are not fully elucidated yet. Here, we demonstrated that endoplasmic reticulum (ER) stress induced *CAP2* expression, and which promoted migration and invasion of liver cancer cells. We also found that the ER stress-induced CAP2 expression is mediated through activation of protein kinase C epsilon (PKCε) and the promotor binding of activating transcription factor 2 (ATF2). In addition, we further demonstrated that *CAP2* expression promoted epithelial-mesenchymal transition (EMT) through activation of Rac1 and ERK. In conclusion, we suggest that ER stress induces *CAP2* expression promoting EMT in liver cancer cells. Our results shed light on the novel functions of *CAP2* in the metastatic process of liver cancer cells.

Keywords: activating transcription factor 2, cyclase-associated protein 2, endoplasmic reticulum-stress, epithelial-mesenchymal transition, extracellular signal-regulated kinase, hepatocellular catcinoma, protein kinase C epsilon

INTRODUCTION

Hepatocellular carcinoma (HCC) is one of the most malignant tumors harboring huge molecular heterogeneity (Woo et al., 2017). Development of HCC is progressed stepwisely from liver cirrhosis, dysplastic nodules, and to early and progressed HCCs (Ojima et al., 2016). Previously, by performing gene expression profiling of the multi-step hepatocarcinogenesis, we identified potential driver genes that drive the multi-step progression of liver cancer (Jee et al., 2019). Among them, *Cyclase-associated protein* 2 (*CAP2*) was found as one of candidate drivers which showed stepwise expression during malignant conversion of pre-cancerous dysplastic lesions to early HCC.

CAP2 protein is highly conserved between yeast and mammal and plays a role in mediating the dynamics of actin polymerization by binding to adenylyl cyclase and binding to G-actin (Kosmas et al., 2015). There are two homologs of *CAP1* and *CAP2*; *CAP1* is expressed ubiquitously, whereas *CAP2* is expressed only in brain, heart, skeletal muscle, and skin (Kosmas et al., 2015). *CAP2* has also been suggested to express in various types of cancers including thyroid, kidney, bladder, and liver cancers. In particular, consistent with our finding, *CAP2* is expressed in 70%-100% of early HCCs, but only in 5%-10% precancerous lesions (Sakamoto, 2009). *CAP2* expression was generally increased as HCC evolves

Received 3 February, 2021; revised 11 May, 2021; accepted 23 May, 2021; published online 23 July, 2021

eISSN: 0219-1032

from early to advanced stages (Fu et al., 2015; Ojima et al., 2016; Sakamoto et al., 2008; Shibata et al., 2006). Moreover, CAP2 expression was significantly associated with overall survival and disease-free survival of HCC patients (Fu et al., 2015). It also has been shown that *CAP2* could promote invasion of HCC cells (Effendi et al., 2013). These studies and ours consistently support that CAP2 expression play an important role in liver cancers. However, underlying mechanisms of *CAP2* expression and its functions in liver cancer cells are not fully elucidated yet. With this concern, in this study, we aimed to investigate the functional roles of *CAP2* in liver cancer progression.

In addition, we have suggested that endoplasmic reticulum (ER) is increased in dysplastic nodules of liver, and which may contribute to the oncogene expression that drives malignant conversion of the pre-cancerous lesions (Jee et al., 2019). ER stress causes unfolded protein responses (UPR) that trigger homeostatic recovery or cell death (Madden et al., 2019; Urra et al., 2016). Enhanced UPR apparently mediates the paradoxical microenvironment in cancers, giving rise to aggressive behaviors of cancer cells (Yadav et al., 2014). In this study, we could demonstrate that the ER stress induces *CAP2* expression in HCC cells, which may provide new insights on the functions of CAP2 in HCC progression.

MATERIALS AND METHODS

Cells, antibodies, and other reagents

Human liver cancer cells of SNU423 (catalog No. KCLB00423) and Huh7 cells (catalog No. KCLB60104) were purchased from Korean Cell Line Bank (KCLB, Korea) and cultured in DMEM (catalog No. 11965084; Invitrogen, USA) supplemented with 10% fetal bovine serum (FBS) (catalog No. 12483-020; Invitrogen), 100 U/ml penicillin, and 100 μg/ml streptomycin (catalog No. 15140122; Invitrogen). Human liver cell (THLE-2 cell) was purchased from ATCC (catalog No. CRL-2706; ATCC, USA) and cultured in BEGM supplemented with growth factors (catalog No. CC3170; Lonza, USA). Mycoplasma tests were performed regularly with polymerase chain reaction (PCR) analysis (e-Myco; COSMO GENETECH, Korea). Authentication of the cell lines were described in Supplementary Information 1-3.

Anti-ERK (1:1,000, catalog No. 9102), anti-phospho-ERK (T202/Y204) (1:1,000, catalog No. 9101), anti-AKT (1:1,000, catalog No. 9272), anti-phospho-AKT (S473) (1:1,000, catalog No. 4060), anti-phospho-SAPK/JNK (T183/Y185) (1:1,000, catalog No. 4668), anti-p38 (1:1,000, catalog No. 9212), anti-phopho-p38 (T180/Y182) (1:1,000, catalog No. 4511), anti-PKCε (1:1,000, catalog No. 2683), anti-phospho-threonine (1:1,000, catalog No. 9386), anti-vimentin (1:1,000, catalog No. 5741), anti-E-cadherin (1:1,000, catalog No. 3195), and anti-ATF2 (1:1,000, catalog No. 35031), anti-mouse IgG, HRP-linked antibody (1:1,000, catalog No. 7076), anti-rabbit IgG, HRP-linked antibody (1:1,000, catalog No. 7074), and Dylight594 Phalloidin (1:20, catalog No. 12877) were purchased from Cell Signaling Biotechnology (USA). Anti-phospho-PKCε (S729) (1:1,000, catalog No. ab63387), anti-N-cadherin (1:1,000, catalog No. ab76057), and anti-snail (1:1,000, catalog No. ab180714) antibodies were from Abcam (UK), anti-CAP2 (1:1,000, catalog No. sc-100916), anti-SAPK/JNK (1:1,000, catalog No. sc-7345), and anti-β-actin (1:1,000, catalog No. sc-47778) antibodies were from Santa Cruz Biotechnology (USA), and anti-Rac1 antibody (1:1,000, catalog No. PA1-091), donkey anti-mouse IgG (H+L) antibody, alexa fluor 488 (1:500, catalog No. R37114), and donkey anti-rabbit IgG (H+L) antibody, alexa fluor 594 (1:500, catalog No. R37119) was from Invitrogen. SB203580 (catalog No. S8307), GF109203X (catalog No. G2911), thapsigargin (catalog No. T9033), tunicamycin (catalog No. T7765), SP600125 (catalog No. S5567), and dithiothreitol (DTT) (catalog No. D9779) were from Sigma-Aldrich (USA), U0126 (catalog No. 662005) was from MERK (Germany), and NSC23766 (catalog No. 2161) was from TOCRIS (USA).

Gene expression constructs and lentiviral vector transfection

Lentiviral constructs expressing *CAP2* shRNAs were purchased from Dharmacon (USA). The *CAP2* (NM_001363533.1), *Rac1*-wild type (Rac1-WT, NM_006908.5)-HA cDNA constructs were cloned into pCDH-CMV-MCS-EF1-Puro using Infusion HD cloning kit (catalog No. 011614; Clontech, Japan), a lentiviral vector for cDNA expression (catalog No. CD510-1; System Biosciences, USA). Rac1-Q61L-HA and Rac1-N17-HA were constructed by site-directed mutagenesis using Rac1-WT as a template. The constructs were used to make stable cell lines as described (Yoon et al., 2019). The targets of *CAP2* shRNAs and the PCR primers were summarized in Supplementary Table S1 and S2. The human *CAP2* promoter sequence was amplified from SNU423 genomic DNA. The 2.5 kb-length clone (–2,500/+100 bp) and truncated derivatives (–2,000/+100, –1,500/+100, –1,000/+100, –500/+100) were obtained using the following. All promoter constructs were cloned into the pGL3-basic luciferase reporter (catalog No. E1751; Promega, USA) vector using Infusion HD cloning kit (Clontech) and verified by DNA sequencing analysis. The candidate ATF2 binding sequences (-2185ATGACGTTAA-2176) of pGL3-CAP2 (–2.5 kb) were mutated using site-directed mutagenesis and verified by DNA sequencing. The putative transcription factor binding sites were analyzed by the PROMO computer program (http://alggen.lsi.upc.es/cgi-bin/promo_v3/promo/promoinit.cgi?dirDB=TF_8.3) (Farre et al., 2003).

siRNA-mediated knockdown

Knockdown experiments for *ATF2* or *PKCε* were performed using 100 nM of negative control siRNA (*siNeg*, catalog No. sc-37007; Santa Cruz Biotechnology), *siATF2* (catalog No. sc-29205; Santa Cruz Biotechnology) or *siPKCε* (catalog No. sc-36251; Santa Cruz Biotechnology). The siRNAs were transfected into liver cancer cells using Lipofectamine 3000 (catalog No. L3000015; Invitrogen). After 48 h of transfection, the cells were harvested for further study.

Luciferase reporter assay

Huh7 cells were plated in 6-well plates and transfected on the following day using Lipofectamine 3000 (Invitrogen). To investigate the *CAP2* promoter region, the cells were

co-transfected with pGL3-basic vector (Promega) or various reporter constructs with a deletion or point mutant of *CAP2* promoter, and pTurbo-GFP plasmid (catalog No. SHC003; Sigma-Aldrich) for normalization of transfection efficiency. After 24 h of transfection, the cells were treated with thapsigargin (100 nM, catalog No. T9033; Sigma-Aldrich) for 24 h and analyzed the luciferase expression using real-time reverse transcription-PCR (qRT-PCR). The relative luciferase expressions were calculated as a fold of induction compared with the pGL3-basic vector control or an unstimulated vector control. All luciferase expression data were normalized with that of *GFP* mRNA.

Chromatin immunoprecipitation (ChIP) assay

Huh7 cells were grown overnight in 150-mm dishes to ~70% confluency, and the cells were treated with or without 100 nM thapsigargin (Sigma-Aldrich) for 24 h. At this time, cells were cross-linked with formaldehyde, harvested, and chromatin immunoprecipitations were performed. ChIP assay was performed using a SimpleChIP Enzymatic Chromatin IP kit (catalog No. 9003) from Cell Signaling Technology.

Immunoprecipitation was performed using a polyclonal antibody against ATF2 (catalog No. 35031; Cell Signaling Technology). As a positive control, an antibody of Histone H3 (catalog No. 4620; Cell Signaling Technology) was used to precipitate the histone-bound *RPL30* promoter (catalog No. 7014; Cell Signaling Technology). The recovered DNA was analyzed by PCR with primers flanking the putative transcription factor binding sites as indicated. As a negative control, we used normal rabbit IgG (catalog No. 2729; Cell Signaling Technology). The primers used for PCR of the ChIP fragents are shown in Supplementary Table S2.

Rac1 GTPase activity assay

Rac1 activity was measured by using a Rac Activation Assays kit (catalog No. STA-401-1; Cell Biolabs, USA). Briefly, the cell lysates were incubated with agarose beads coupled to the p21-binding domain (PBD) of p21-activated protein kinase (PAK). The amount of bound form Rac1 was measured by western blot analysis using an anti-Rac1 antibody.

Real-time qPCR

Cells were harvested and total RNAs were isolated using an RNeasy kit (catalog No. 74104; Qiagen, Netherlands). The PrimeScript RT kit (catalog No. RR037A; Takara, Japan) was used to reverse transcribe the 1 μg total RNA into cDNA. PCR was done using a CFX96 Real Time PCR Detection System (Bio-Rad) with IQ SYBR Green Supermix (catalog No. BR170-8882; Bio-Rad). Analysis of each sample was performed at least three times for each experiment, and the data were presented as the average values of $2^{-\Delta\Delta CT}$ ± SD. The sequences of primers are shown in Supplementary Table S2.

Immunoprecipitation and Western blots

For immunoprecipitation, 500 μg of proteins were incubated overnight with anti-ATF2 antibody (catalog No. 35031, 1:100; Cell Signaling Technology), subsequently with protein A/G agarose beads (catalog No. sc-2003; Santa Cruz Biotechnology) for 1 h. The beads were washed five times from which immuno-precipitates were extracted with 2 × SDS sample buffer.

For preparing total cell lysates, cells were lysed in lysis buffer (20 mM Tris-HCl [pH 8.0], 1% Triton X-100, 2 mM EDTA, and 1 mM phenylmethylsulfonyl fluoride), incubated on ice for 20 min, and centrifuged for 20 min to remove cell debris. A total of 20 μg of whole-cell lysate was used in SDS-polyacrylamide gel electrophoresis. The proteins were then electro-transferred to a nitrocellulose membrane and incubated overnight with antibodies at 4°C. Then, the membranes were incubated with peroxidase-conjugated secondary antibodies (anti-mouse IgG, HRP-linked antibody, catalog No. 7076, 1:1,000 [Cell Signaling Technology]; anti-rabbit IgG, HRP-linked antibody, catalog No. 7074, 1:1,000 [Cell Signaling Technology]) for 1 h at room temperature, and the signal was detected using an enhanced chemiluminescence detection kit (catalog No. 34580; PIERCE, USA).

Confocal microscopy

To demonstrate the localization of proteins, cells were grown on Lab-Tek four-well glass chamber slides (catalog No. C6807; NUNC, USA). After 24 h incubation, cells were fixed and permeabilized with cold methanol for 5 min, washed with phosphate-buffered saline (PBS), and incubated with primary antibody (1:100) and secondary antibody conjugates (1:500). Images were collected on a laser scanning confocal microscope LSM710 (Carl Zeiss, Germany) equipped with argon (488 nm) and krypton (568 nm) lasers, using a 40 × water immersion objective lens. Images were processed with ZEN 2009 light edition (Carl Zeiss).

Cell proliferation

Cells (5×10^3) were split into 96-well plates and incubated in media containing 10% FBS for 48 h. Cell proliferation was measured by WST-1 assay (catalog No. 05015944001; Roche, Korea). Each experiment was performed in four replicates at least three times.

Cell migration/invasion assay

Cell migration/invasion assay were performed in 24-well modified Boyden chamber (8-μm pore size, catalog No. 3422 Costar; Corning Life Sciences, USA). For invasion assay, the Transwell filter inserts were coated with collagen type I (catalog No. A10644-01; Invitrogen). In the migration assay, 1×10^5 cells in 0.2 ml of serum-free DMEM were seeded into the upper chamber insert. The lower chamber was filled with 0.6 ml DMEM/10% FBS. After 6 h, cells at the membrane undersurface were fixed, stained. The images were captured by light microscope (magnification, ×5). For spectrophotometric analysis, the crystal violet-stained cells were solubilized with 200 μl 10% acetic acid (v/v, catalog No. 414; Duksan Pure Chemicals, Korea) for 15 min. The absorbance at 570 nm of the extracts (50 μl) was measured with by a spectrophotometer (96-well plate reader).

Wound healing assay

Cell motility was measured by wound healing assay. Cells (8×10^5) were split into 60 mm dishes and incubated in media containing 10% FBS for 24 h. Cells were cultured until

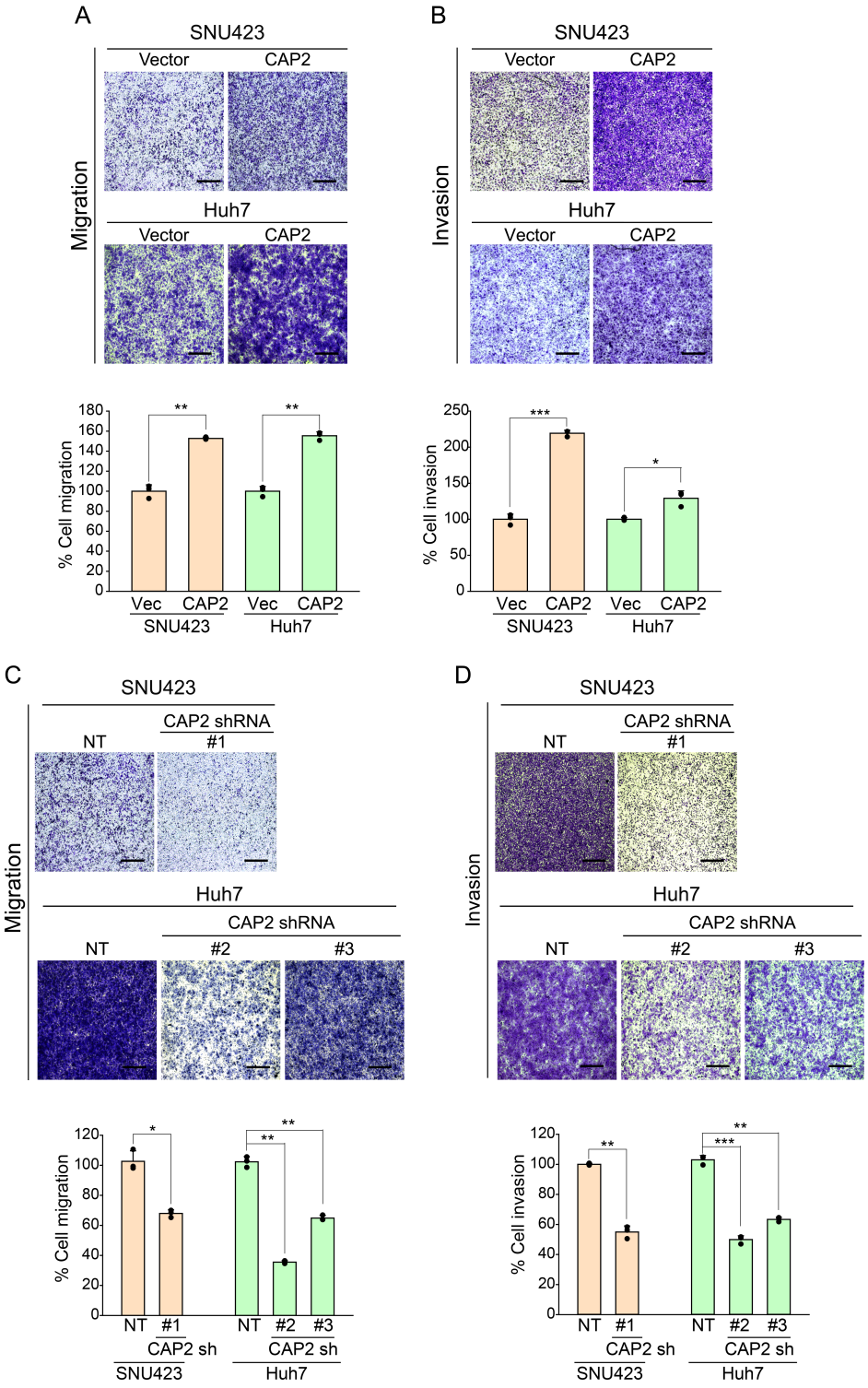

Fig. 1. *CAP2* increases migration and invasion of liver cancer cells. Migration (A and C) and invasion (B and D) were measured in Transwell migration/invasion assays. Migrated/invaded cells were fixed with 10% formaldehyde and stained with 1% crystal violet. NT, non-targeting control. Images were captured under a light microscope (magnification, ×5). Scale bars = 500 μm. The data are presented as mean ± SEM for triplicate determinations. $*P < 0.05$, $**P < 0.01$, and $***P < 0.001$.

a monolayer form, then scratched with 200 μl tip. The cells were changed to media containing 1% FBS and incubated for 24 h or 48 h. Images were captured using bright field and 4× magnification. The wound width was measured as the average distance between edges of the gap. The scale bar was equivalent in all images and all experiments were performed at least three times for reproducible results.

Statistical analysis

The data were presented as mean ± SEM. Statistical analysis was performed using the SigmaPlot 12.5 software. Differences were assessed by paired Student's *t*-test. All the data were derived from at least three independent experiments.

RESULTS

CAP2 induces migration and invasion but not proliferation of liver cancer cells

We established the *CAP2* overexpression systems using SNU423 (SNU423-*CAP2*) and Huh7 cells (Huh7-*CAP2*) (Supplementary Figs. S1A and S1B). The *CAP2*-overexpressing cells showed higher migration and invasion properties than the Control vector-cells (SNU423-Vector and Huh7-Vector; Fig. 1A and 1B, Supplementary Fig. S2). In addition, we could demonstrate that the shRNA-mediated knockdown of *CAP2* (SNU423-*CAP2 sh* and Huh7-*CAP2 sh*) significantly suppressed the migration and invasion of liver cancer cells (Fig. 1C and 1D, Supplementary Figs. S1C and S2). However, *CAP2* expression did not affect the liver cancer cell proliferation, indicating that CAP2 functions to promote metastasis but not proliferation of the liver cancer cells (Supplementary Fig. S3).

ER stress induces *CAP2* expression through promoter binding ATF2

As we have predicted that *CAP2* expression is induced by ER stress from the transcriptome data analyses, we examined the effects of ER stress modulators on *CAP2* expression. We could demonstrate that the treatment ER stress inducers such as thapsigargin, tunicamycin or DTT can induce the expression of *CAP2* mRNAs and proteins (Fig. 2A and 2B). Induction of ER stress was confirmed by examining the expression of an ER stress marker *GRP78* (Supplementary Fig. S4). We also demonstrated that the thapsigargin treatment could promote invasion of the cancer cells, and which was abolished by knockdown of CAP2 expression (Supplementary Fig. S5). These findings suggest that CAP2 plays a critical role in the ER stress-mediated invasion of liver cancer cells.

In addition, we compared the expression of *CAP2* in normal liver cells (THLE-2 cell) and HCC cells (SNU423 and Huh7 cells), which revealed no significant difference between them. However, unlike the HCC cells, THLE-2 cells did not induce *CAP2* expression by thapsigargin treatment (Supplementary Fig. S6), which may indicate the cancer cell-specific function of *CAP2*.

To further investigate the underlying molecular mechanisms of the ER stress-mediated *CAP2* expression, we cloned the 5`-flanking region of the *CAP2* gene using the template genomic DNA of SNU423. The sequence of this 5`-flanking region encompassed residues −2.5 kb to +100 bp relative to the putative transcription start site. The promoter activity of these regions was measured by generating a set of serial deletion constructs by fusing the truncated forms of the 5`-flanking region to the 5`-end of a luciferase reporter gene in the pGL3-basic vector (Fig. 2C). Huh7 cells were transiently transfected with these reporter constructs and then treated with 100 nM thapsigargin. We found that the construct containing the −2.5 kb to +100 bp fragment showed the highest promoter activity under ER stress condition. Deletion of the 5`-region could abolish the promoter activity (Fig. 2D). These results suggest that the −2.5 kb to −2.0 kb region contains the binding site for cis-responsive element which is required for the *CAP2* expression by ER stress.

Next, we computationally predicted the binding of ATF2 (activating transcription factor 2) to this promotor site by using PROMO software. To validate this prediction result, we performed a site-directed mutagenesis experiment, which revealed that the mutations at the ATF2 binding site significantly reduced the promoter activity (Fig. 2E). In addition, we further confirmed the binding of ATF2 with *CAP2* promoter region by performing a chromatin immunoprecipitation (ChIP) experiment. We could observe the enriched immunoprecipitated chromatins in the PCR products using *CAP2* promoter-specific primers (ChIP-1 primer and ChIP-2 primer). Moreover, thapsigargin treatment could enhance the binding of ATF2 and *CAP2* promoter (Fig. 2F). As a negative control, PCR reactions were performed with the primers (ChIP-2 primers) for the 2.5 kb downstream region of the ATF2 binding site of *CAP2*, which showed no immunoprecipitation. We also demonstrated that knockdown of *ATF2* suppressed the thapsigargin-induced *CAP2* expression in liver cancer cells (Supplementary Fig. S7, Fig. 2G and 2H). Taken together these results, we suggest that ER stress-induced *CAP2* expression is mediated through the promoter binding of ATF2.

PKCε is involved in ER stress-mediated ATF2 activation

ATF2 is activated by several stress-activated protein kinases such as ERK1, JNK, p38, and protein kinase epsilon (PKCε) in response to a variety of stimuli (Lau and Ronai, 2012). Thus, we examined these protein kinases in the ER stress-induced liver cancer cells, which revealed that the thapsigargin treatment could activate ERK, JNK, p38, and PKCε (Fig. 3A). We also evaluated the effects of the inhibitors of stress-activated protein kinases. The PKCε inhibitor GF109203X reduced stress-induced *CAP2* transcription but did not the other inhibitors of ERK1 (U0126, 20 μM), JNK (SP600125, 25 μM), and p38 (SB203580, 10 μM) (Fig. 3B, Supplementary Fig. S8). These results may indicate that only *PKCε* is involved in the ER stress-mediated ATF2 activation. We further confirmed this finding by evaluating the effect of siRNA-mediated knockdown of *PKCε* (*siPKCε*), which could suppress the thapsigargin-mediated *CAP2* expression (Supplementary Fig. S9, Fig. 3C). Treatment of *siPKCε* could also suppress the ATF2 activation by thapsigargin treatment (Fig. 3D). Thus, we suggest that PKCε is involved in ER stress-mediated ATF2 activation.

CAP2 induces EMT in liver cancer cells via Rac1-ERK activation

As EMT has been addressed to induce the migration and invasion of cancer cells, we evaluated whether CAP2 expression can induce EMT by examining the expression of the EMT markers such as the suppression of E-cadherin and cytokeratin and the expression of vimentin, N-cadherin, twist, snail, and slug (Ahmed et al., 2020; Zeisberg and Neilson, 2009). We could observe that the CAP2-overexpressing cells induced EMT, showing higher expression of vimentin, N-cadherin, and snail, but lower expression of E-cadherin (Fig. 4A). Moreover, we also found that the *CAP2*-overexpressing cells enhanced the expression of the active form ERK (Fig. 4B). Treatment of an ERK inhibitor (U0126, 20 μM) suppressed the expression levels of vimentin, N-cadherin, and snail (Fig.

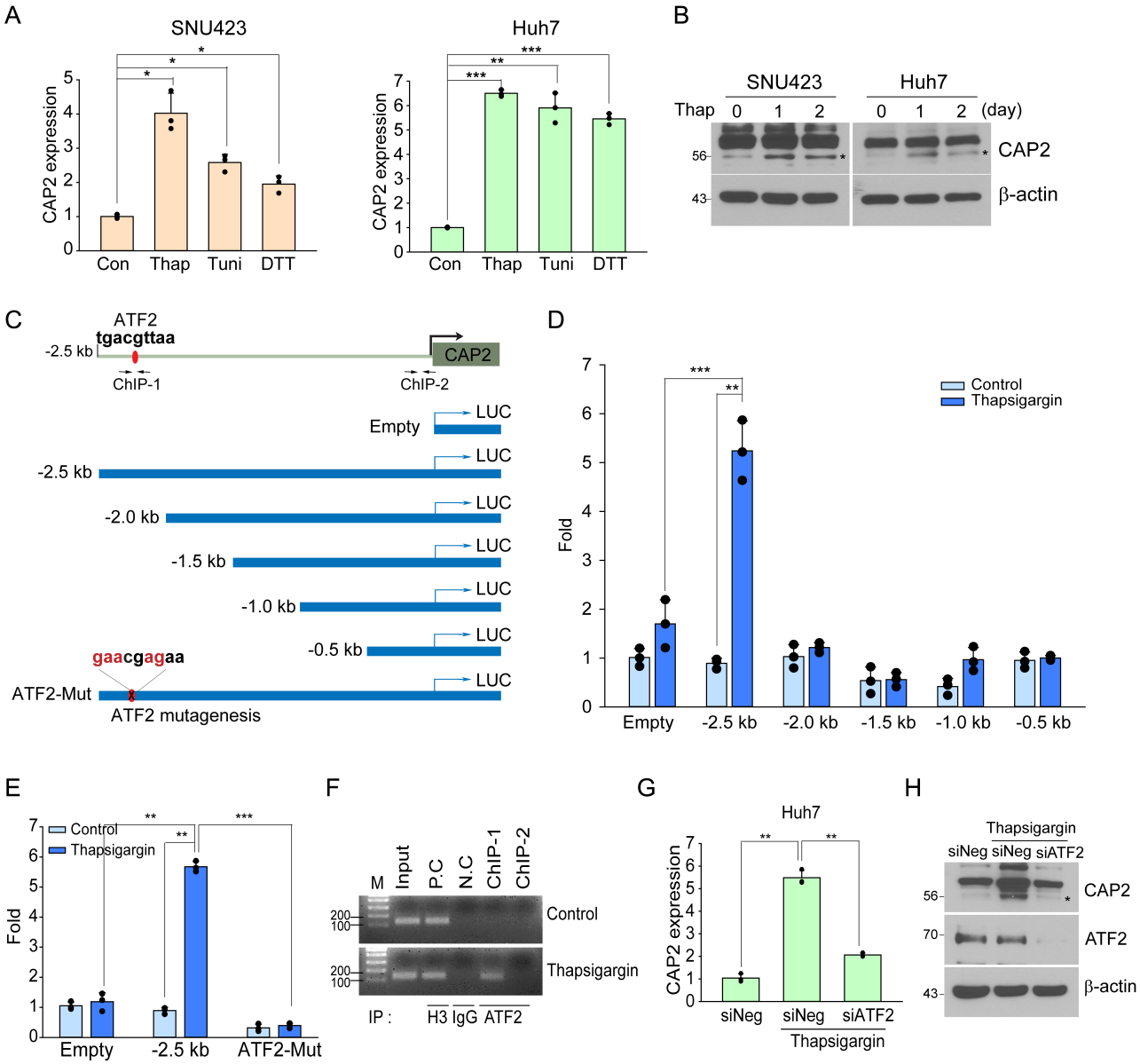

Fig. 2. ER stress induces *CAP2* expression via promoter binding of ATF2. (A) SNU423 and Huh7 cells are treated with/without thapsigargin (Thap; 50 nM and 100 nM, respectively), tunicamycin (Tuni; 50 ng/ml), or DTT (1 mM) for 24 h. Con, control. Expression of *CAP2* mRNA is measured by qRT-PCR and normalized to β-actin mRNA. Data represent mean ± SEM of 4 independent experiments. (B) SNU423 and Huh7 cells are treated with thapsigargin (50 nM or 100 nM, respectively) for indicated times. Cell lysates are examined by western blotting with the indicated antibodies. CAP2 is indicated by asterisks (*). (C) Schematic representation of the *CAP2* luciferase reporters. ChIP primer sets are shown. (D and E) Huh7 cells are transiently co-transfected with pTurbo-GFP and deleted constructs (D) or ATF2 binding site mutated construct (ATF2-Mut) (E) of the *CAP2* promoter. After treatment with 100 nM thapsigargin for 24 h, total RNAs are extracted. Luciferase expression is monitored by qRT-PCR; Luciferase expression levels are normalized by that of *GFP* mRNA (right). Data represent mean ± SEM of the three independent experiments. (F) Cross-linked chromatin preparation from control and thapsigargin (100 nM, 24 h) treated cells are immunoprecipitated with anti-ATF2, anti-Histone H3 (H3), or normal rabbit IgG (IgG) antibodies. The ATF2 binding sites on the immunoprecipitated DNA are determined by RT-PCR using their corresponding primers. Amplificons of the input chromatin (input) prior to immunoprecipitation were served as controls for each chromatin extraction and PCR amplification. Chromatin immunoprecipitation using a Histone H3 antibody is served as a positive control (P.C) and a non-specific antibody (normal rabbit IgG) is served as a negative control (N.C). (G and H) Huh7 cells are transiently transfected with siNegative control (*siNeg*) or *siATF2*. After 24 h, thapsigargin (100 nM) is treated for 24 h and the *CAP2* expression levels are measured by qRT-PCR (G) and western blotting (H). CAP2 is indicated by asterisk (*). The data represent mean ± SEM of three independent experiments. $*P < 0.05$, $**P < 0.01$, and $***P < 0.001$.

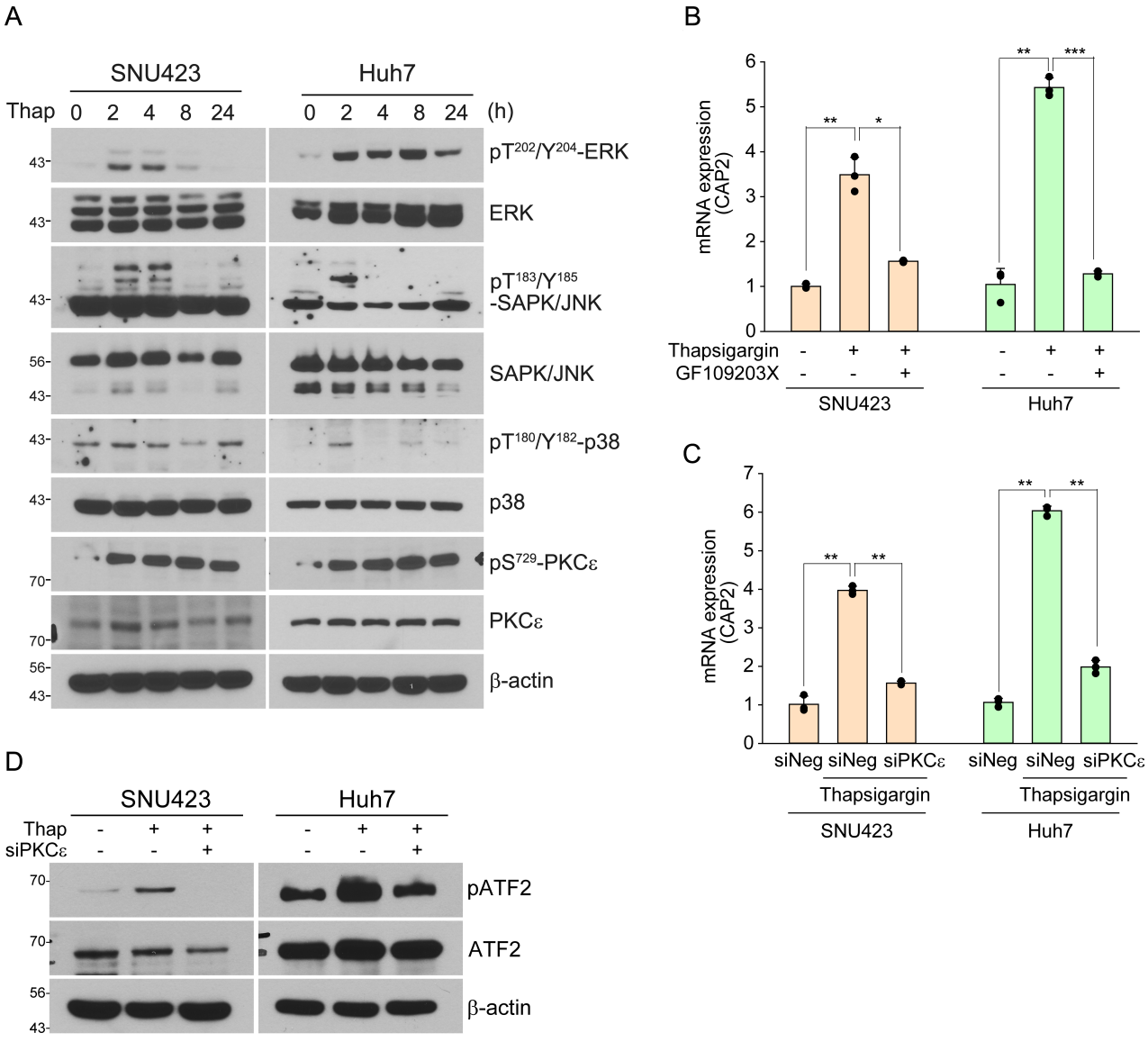

Fig. 3. PKCε is involved in the ER stress-induced ATF2 activation. (A) SNU423 and Huh7 cells are treated with thapsigargin (Thap; 50 nM and 100 nM, respectively) for the indicated times and cell lysates are examined by western blotting with the indicated antibodies. (B) SNU423 and Huh7 cells are treated with thapsigargin (50 nM and 100 nM, respectively) alone or with thapsigargin plus the PKCε inhibitor GF109203X (GF, 20 μM) for 24 h. Relative expression of *CAP2* mRNA is measured by qRT-PCR. Data represent mean ± SEM of 3 independent experiments. (C and D) SNU423 and Huh7 cells are transiently transfected with siNegative control (*siNeg*) or *siPKCε* and after 24 h, thapsigargin (100 nM) is treated for 24 h. *CAP2* expression is measured by qRT-PCR. Data represent mean ± SEM of three independent experiments (C). ATF2 activation is monitored by western blotting with the indicated antibodies (D). $*P < 0.05$, $**P < 0.01$, and $***P < 0.001$.

4C). These results strongly suggest that *CAP2* can induce EMT in liver cancer cells, and which is mediated by activation of ERK.

In addition, CAP2 has been addressed to play an important role in actin dynamics (Kosmas et al., 2015). Indeed, in the *CAP2*-overexpressing cells, we could observe the localized expression of CAP2 protein in the membrane lamellipodia and ruffles, which are the characteristic feature of the actively migrating cells with EMT (Fig. 5A). Moreover, Rac1 is suggested to regulate these membrane features by converting F-actin filaments into G-actin monomers, and which is mediated by activation of p21-activated kinase (PAK)-cofilin signaling pathway (Bid et al., 2013). In fact, Rac1-ERK pathway has been suggested to play important roles in cell migration and invasion (Ebi et al., 2013; Jiang et al., 2014; Lin et al., 2018; Pang et al., 2020). With this concern, we could observe that the formation of F-actin filaments was decreased by the overexpression of *CAP2* in liver cancer cells (Fig. 5A). Moreover, CAP2 and Rac1 proteins were co-localized at membrane lamellipodia and ruffles, which may imply the involvement of

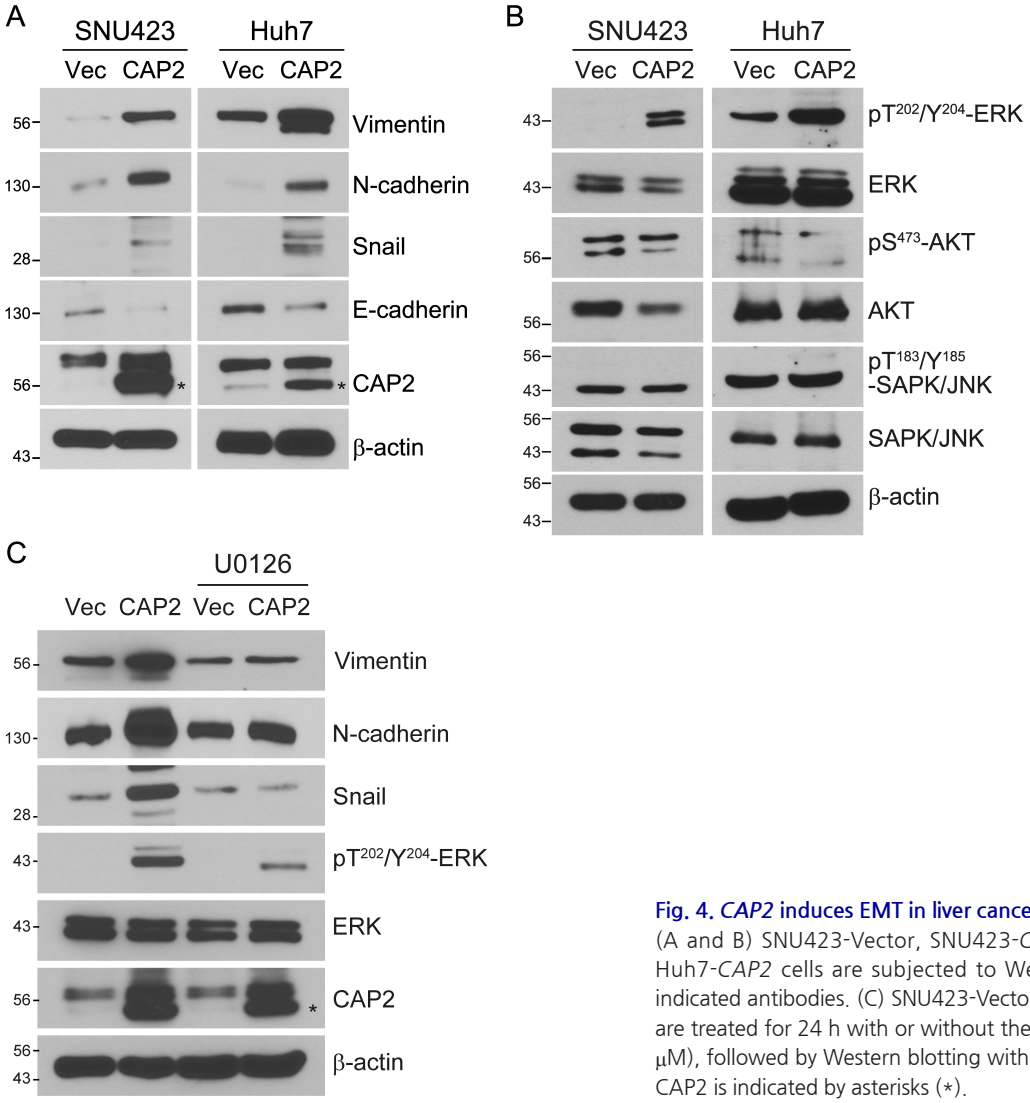

Fig. 4. *CAP2* induces EMT in liver cancer cells via ERK activation. (A and B) SNU423-Vector, SNU423-*CAP2*, Huh7-Vector, and Huh7-*CAP2* cells are subjected to Western blotting with the indicated antibodies. (C) SNU423-Vector and SNU423-*CAP2* cells are treated for 24 h with or without the ERK inhibitor U0126 (20 μM), followed by Western blotting with the indicated antibodies. CAP2 is indicated by asterisks (*).

Rac1 in the CAP2-mediated EMT (Fig. 5B). We could validate the interaction of CAP2 and Rac1 by a pull-down experiment using the GST linked to the Rac1 effector PAK (Fig. 5C). Also, we could demonstrate that the treatment of a Rac1 inhibitor (NSC23766, 50 μM) suppressed the ERK activity and the expression of EMT biomarkers such as vimentin, N-cadherin, and snail (Fig. 5D). We further validated these findings by generating the *CAP2*-expresing cells with different forms of Rac1, i.e., *Rac1* wild-type HA (*Rac1*-WT), dominant-positive mutant *Rac1*-Q61L-HA (*Rac1*-Q61L), dominant-negative mutant *Rac1*-N17-HA (*Rac1*-N17), or control vector (Vector) (Fig. 5E). As expected, the *CAP2*-expressing cells with *Rac1*-WT and *Rac1*-Q61L exhibited the increased protein levels of vimentin, N-cadherin, and snail. By contrast, the *CAP2*-expressing cells with *Rac1*-N17 exhibited the decreased levels of the ERK activity as well as those EMT proteins.

Furthermore, the *Rac1*-WT or the *Rac1*-Q61L-expressing cells showed the increased migration and invasion, whereas the *Rac1*-N17-expressing cells showed the reduced migration and invasion compared to those of the Vector cells (Fig. 5F). Treatment of an ERK inhibitor U0126 (20 μM) did not affect the ER stress-induced *CAP2* expression, indicating that ERK is a downstream effector of CAP2 (Supplementary Fig. S10). Taken together these results, we suggest that *CAP2* induces EMT via Rac1 and ERK activation.

DISCUSSION

In this study, we demonstrated that ER stress induces CAP2 expression, and which facilitated EMT promoting migration and invasion of liver cancer cells. We also demonstrated that PKCε-ATF2 signaling is involved in ER stress-induced *CAP2* expression.

Cancer cells can survive in micro-environmental conditions that cause ER-stress. The ability to tolerate constant ER stress improves cancer cell survival, angiogenesis, metastatic ability, drug resistance, and immune suppression (Cubillos-Ruiz et al., 2017). ER stress promotes UPR that controls the balance

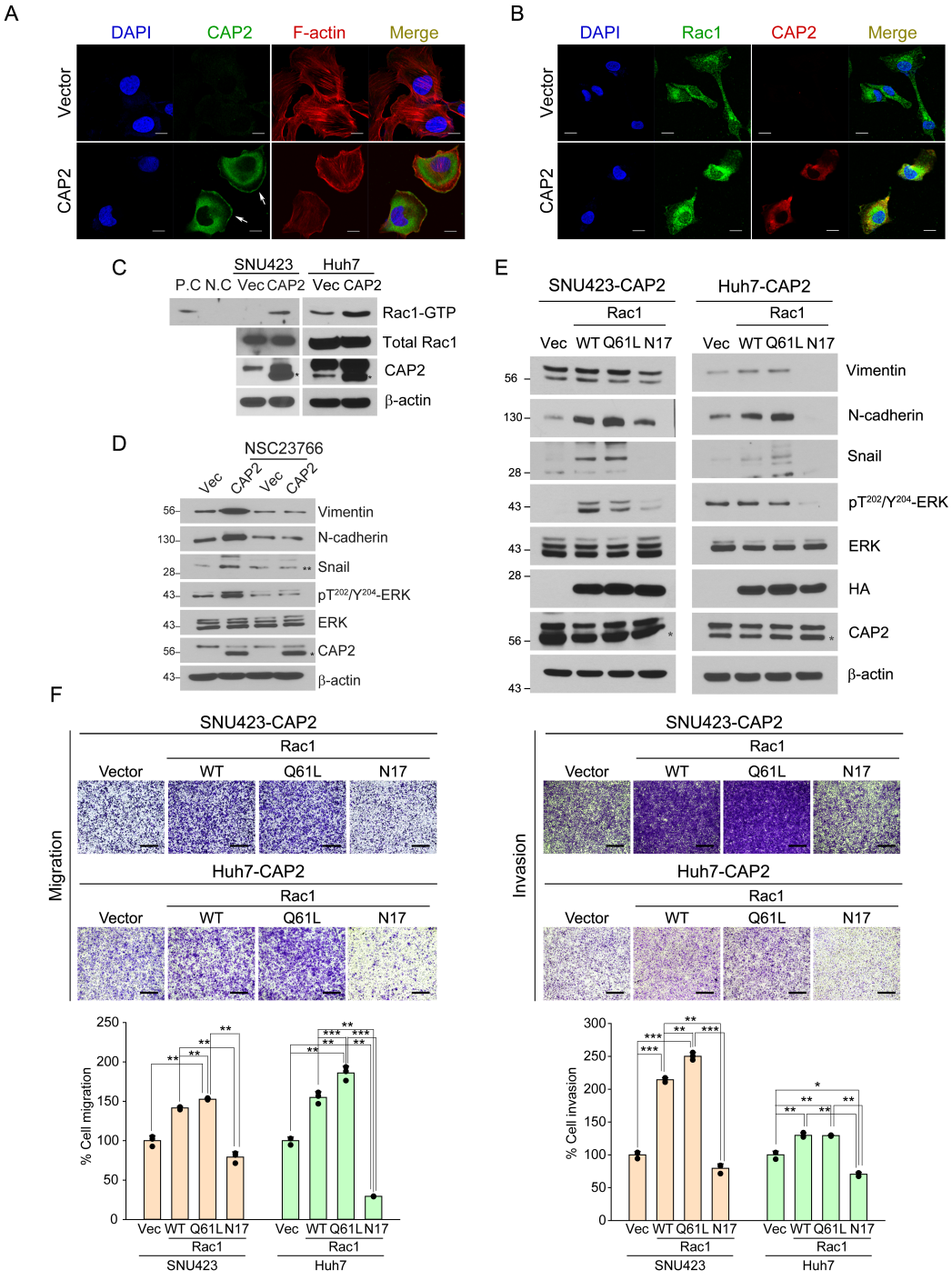

Fig. 5. Rac1 is involved in *CAP2*-mediated ERK activation and EMT. (A and B) SNU423-Vector and SNU423-*CAP2* cells are stained with the indicated fluorescent antibodies. Nuclei are counter-stained with DAPI. Images are captured under a laser scanning confocal microscope (×40). White arrows indicate membrane ruffles. Scale bars = 10 μm. (C) Total cell lysates prepared from the indicated cells are incubated with agarose beads coupled to PAK PBD. Bound Rac1 is detected with Western blotting using a Rac1 Ab (upper panel). The amount of total Rac1 is also measured (lower panel). P.C, positive control; N.C, negative control. Asterisks (*) indicate CAP2. (D) SNU423-Vector and SNU423-*CAP2* cells were treated for 24 h with NSC23766 (50 μM) and subjected to western blotting with the indicated antibodies. Asterisk (*) indicates CAP2, double asterisk (**) indicates Snail. (E) SNU423-*CAP2* and Huh7-*CAP2* cells stably expressing Vector (Vec), *Rac1*-WT, *Rac1*-Q61L, or *Rac1*-N17 are subjected to Western blotting with the indicated antibodies. Asterisks (*) indicate CAP2. (F) Migration and invasion of the indicated cells were measured in Transwell assays. Migrated/invaded cells are fixed with 10% formaldehyde and stained with 1% crystal violet. WT, wild type. Images are captured under a light microscope (magnification, ×5). Scale bars = 500 μm. Data are presented as mean ± SEM for triplicate experiments. $*P < 0.05$, $**P < 0.01$, and $***P < 0.001$.

between cell survival and cell death, playing critical roles in cancer cell adaptation to stress and cancer development (Sisinni et al., 2019; Wang and Kaufman, 2014). We found that *CAP2* is one of downstream effector molecules that respond to ER stress in liver cancer cells. Moreover, we successfully demonstrated that the CAP2 expression was localized in the lamellipodia and ruffles of liver cancer cells indicating EMT (see Figs. 2 and 5A). We also suggested that Rac1-ERK signaling is involved in the CAP2-mediated EMT. Rac1 is a GTP-binding protein which has been known to regulate actin cytoskeleton reorganization to form cell surface extensions (lamellipodia/ruffles) through ERK activation (Bright et al., 2018; De et al., 2019; Ebi et al., 2013; Jiang et al., 2014; Lin et al., 2018; Pang et al., 2020). ERKs act as critical regulators of cell proliferation by promoting cell cycle progression. However, in some systems, hyperactivation of ERKs by the expression of the activated forms of Ras, Raf, or MEK1 causes cell cycle arrest, promoting mesenchymal transition with increased cell migration and invasion (Meloche and Pouyssegur, 2007; Murphy and Blenis, 2006; Shin et al., 2019). Consistently, we could demonstrate that the activation of CAP2 induced EMT but not proliferation of liver cancer cells, and which was mediated through Rac1 and ERK activation (see Figs. 4 and 5). These results may suggest that the metastasis of cancer cells might be controlled by stage-specific fine modulation of ERK activity, although further mechanism studies are required.

In conclusion, although our study was limited to *in vitro* experiments, we could successfully demonstrate that ER stress-mediated *CAP2* expression plays a critical role in the metastatic process of liver cancer cells. We suggest that targeting CAP2 and its downstream pathways can be a new therapeutic strategy for treatment of HCC patients.

Note: Supplementary information is available on the Molecules and Cells website (www.molcells.org).

ACKNOWLEDGMENTS

This work was supported by grants from the National Research Foundation of Korea (NRF), funded by the Korean government (MSIP) (NRF-2017R1E1A1A01074733, NRF-2017M3A9B6061509, NRF-2017M3C9A6047620, NRF-2019R1A5A2026045, and NRF-2019R1I1A1A01057206).

AUTHOR CONTRIBUTIONS

S.Y. performed experiments and wrote the manuscript. B.S. performed experiments. H.G.W. contributed to overall study design, wrote the manuscript, and directed the study.

CONFLICT OF INTEREST

The authors have no potential conflicts of interest to disclose.

ORCID

Sarah Yoon https://orcid.org/0000-0002-4031-582X
Boram Shin https://orcid.org/0000-0003-0251-0576
Hyun Goo Woo https://orcid.org/0000-0002-0916-893X

REFERENCES

Ahmed, M.B., Islam, S.U., Sonn, J.K., and Lee, Y.S. (2020). PRP4 kinase domain loss nullifies drug resistance and epithelial-mesenchymal transition in human colorectal carcinoma cells. Mol. Cells *43*, 662-670.

Bid, H.K., Roberts, R.D., Manchanda, P.K., and Houghton, P.J. (2013). RAC1: an emerging therapeutic option for targeting cancer angiogenesis and metastasis. Mol. Cancer Ther. *12*, 1925-1934.

Bright, M.D., Clarke, P.A., Workman, P., and Davies, F.E. (2018). Oncogenic RAC1 and NRAS drive resistance to endoplasmic reticulum stress through MEK/ERK signalling. Cell. Signal. *44*, 127-137.

Cubillos-Ruiz, J.R., Bettigole, S.E., and Glimcher, L.H. (2017). Tumorigenic and immunosuppressive effects of endoplasmic reticulum stress in cancer. Cell *168*, 692-706.

De, P., Aske, J.C., and Dey, N. (2019). RAC1 takes the lead in solid tumors. Cells *8*, 382.

Ebi, H., Costa, C., Faber, A.C., Nishtala, M., Kotani, H., Juric, D., Della Pelle, P., Song, Y., Yano, S., Mino-Kenudson, M., et al. (2013). PI3K regulates MEK/ERK signaling in breast cancer via the Rac-GEF, P-Rex1. Proc. Natl. Acad. Sci. U. S. A. *110*, 21124-21129.

Effendi, K., Yamazaki, K., Mori, T., Masugi, Y., Makino, S., and Sakamoto, M. (2013). Involvement of hepatocellular carcinoma biomarker, cyclase-associated protein 2 in zebrafish body development and cancer progression. Exp. Cell Res. *319*, 35-44.

Farre, D., Roset, R., Huerta, M., Adsuara, J.E., Rosello, L., Alba, M.M., and Messeguer, X. (2003). Identification of patterns in biological sequences at the ALGGEN server: PROMO and MALGEN. Nucleic Acids Res. *31*, 3651-3653.

Fu, J., Li, M., Wu, D.C., Liu, L.L., Chen, S.L., and Yun, J.P. (2015). Increased expression of CAP2 indicates poor prognosis in hepatocellular carcinoma. Transl. Oncol. *8*, 400-406.

Jee, B.A., Choi, J.H., Rhee, H., Yoon, S., Kwon, S.M., Nahm, J.H., Yoo, J.E., Jeon, Y., Choi, G.H., Woo, H.G., et al. (2019). Dynamics of genomic, epigenomic, and transcriptomic aberrations during stepwise hepatocarcinogenesis. Cancer Res. *79*, 5500-5512.

Jiang, Q.H., Wang, A.X., and Chen, Y. (2014). Radixin enhances colon cancer cell invasion by increasing MMP-7 production via Rac1-ERK pathway. ScientificWorldJournal *2014*, 340271.

Kosmas, K., Eskandarnaz, A., Khorsandi, A.B., Kumar, A., Ranjan, R., Eming, S.A., Noegel, A.A., and Peche, V.S. (2015). CAP2 is a regulator of the actin cytoskeleton and its absence changes infiltration of inflammatory cells and contraction of wounds. Eur. J. Cell Biol. *94*, 32-45.

Lau, E. and Ronai, Z.A. (2012). ATF2 - at the crossroad of nuclear and cytosolic functions. J. Cell Sci. *125*, 2815-2824.

Lin, C.H., Shih, C.H., Lin, Y.C., Yang, Y.L., and Chen, B.C. (2018). MEKK1, JNK, and SMAD3 mediate CXCL12-stimulated connective tissue growth factor expression in human lung fibroblasts. J. Biomed. Sci. *25*, 19.

Madden, E., Logue, S.E., Healy, S.J., Manie, S., and Samali, A. (2019). The role of the unfolded protein response in cancer progression: from oncogenesis to chemoresistance. Biol. Cell *111*, 1-17.

Meloche, S. and Pouyssegur, J. (2007). The ERK1/2 mitogen-activated protein kinase pathway as a master regulator of the G1- to S-phase transition. Oncogene *26*, 3227-3239.

Murphy, L.O. and Blenis, J. (2006). MAPK signal specificity: the right place at the right time. Trends Biochem. Sci. *31*, 268-275.

Ojima, H., Masugi, Y., Tsujikawa, H., Emoto, K., Fujii-Nishimura, Y., Hatano, M., Kawaida, M., Itano, O., Kitagawa, Y., and Sakamoto, M. (2016). Early hepatocellular carcinoma with high-grade atypia in small vaguely nodular lesions. Cancer Sci. *107*, 543-550.

Pang, Y., Zhao, Y., Wang, Y., Wang, X., Wang, R., Liu, N., Li, P., Ji, M., Ye, J., Sun, T., et al. (2020). TNFAIP8 promotes AML chemoresistance by

activating ERK signaling pathway through interaction with Rac1. J. Exp. Clin. Cancer Res. *39*, 158.

Sakamoto, M. (2009). Early HCC: diagnosis and molecular markers. J. Gastroenterol. *44* Suppl 19, 108-111.

Sakamoto, M., Mori, T., Masugi, Y., Effendi, K., Rie, I., and Du, W. (2008). Candidate molecular markers for histological diagnosis of early hepatocellular carcinoma. Intervirology *51* Suppl 1, 42-45.

Shibata, R., Mori, T., Du, W., Chuma, M., Gotoh, M., Shimazu, M., Ueda, M., Hirohashi, S., and Sakamoto, M. (2006). Overexpression of cyclase-associated protein 2 in multistage hepatocarcinogenesis. Clin. Cancer Res. *12*, 5363-5368.

Shin, S., Buel, G.R., Nagiec, M.J., Han, M.J., Roux, P.P., Blenis, J., and Yoon, S.O. (2019). ERK2 regulates epithelial-to-mesenchymal plasticity through DOCK10-dependent Rac1/FoxO1 activation. Proc. Natl. Acad. Sci. U. S. A. *116*, 2967-2976.

Sisinni, L., Pietrafesa, M., Lepore, S., Maddalena, F., Condelli, V., Esposito, F., and Landriscina, M. (2019). Endoplasmic reticulum stress and unfolded protein response in breast cancer: the balance between apoptosis and autophagy and its role in drug resistance. Int. J. Mol. Sci. *20*, 857.

Urra, H., Dufey, E., Avril, T., Chevet, E., and Hetz, C. (2016). Endoplasmic reticulum stress and the hallmarks of cancer. Trends Cancer *2*, 252-262.

Wang, M. and Kaufman, R.J. (2014). The impact of the endoplasmic reticulum protein-folding environment on cancer development. Nat. Rev. Cancer *14*, 581-597.

Woo, H.G., Choi, J.H., Yoon, S., Jee, B.A., Cho, E.J., Lee, J.H., Yu, S.J., Yoon, J.H., Yi, N.J., Lee, K.W., et al. (2017). Integrative analysis of genomic and epigenomic regulation of the transcriptome in liver cancer. Nat. Commun. *8*, 839.

Yadav, R.K., Chae, S.W., Kim, H.R., and Chae, H.J. (2014). Endoplasmic reticulum stress and cancer. J. Cancer Prev. *19*, 75-88.

Yoon, S., Choi, J.H., Kim, S.J., Lee, E.J., Shah, M., Choi, S., and Woo, H.G. (2019). EPHB6 mutation induces cell adhesion-mediated paclitaxel resistance via EPHA2 and CDH11 expression. Exp. Mol. Med. *51*, 1-12.

Zeisberg, M. and Neilson, E.G. (2009). Biomarkers for epithelial-mesenchymal transitions. J. Clin. Invest. *119*, 1429-1437.